2025-06

Stapp Car Crash Journal, Vol. 69, pp. 162-180

Traumatic Head and Brain Injuries in Helmeted Motorcycle Crashes

John Lloyd, PhD, CPE, ACTAR [1]

[1] BRAINS, Inc., 32824 Michigan Avenue, San Antonio, Florida 33576

ABSTRACT – This study presents an analysis of 364 motorcycle helmet impact tests, including standard certified full-face, open-face, and half-helmets, as well as non-certified (novelty) helmet designs. Two advanced motorcycle helmet designs that incorporate technologies intended to mitigate the risk of rotational brain injuries (rTBI) were included in this study. Results were compared to 80 unprotected tests using an instrumented 50th percentile Hybrid III head form and neck at impact speeds ranging from 6 to 18 m/s (13 to 40 mph).

Results show that, on average, the Head Injury Criterion (HIC) was reduced by 92 percent across certified helmets, compared to the unhelmeted condition, indicating substantial protection against focal head and brain injuries. However, findings indicate that standard motorcycle helmets increase the risk of AIS 2 to 5 rotational brain injuries (rTBI) by an average of 30 percent compared to the unprotected condition, due to the increased rotational inertia generated by the added size and weight of the helmet. Advanced helmets performed, on average, about 5 percent better than standard certified helmets. Non-certified or novelty helmets offer inadequate protection against focal head and brain injuries, though they may offer some insight into rTBI protection.

The findings of this study also indicate a critical methodological deficiency in the oblique impact tests utilized in revised motorcycle helmet standards, including ECE 22.06, Snell M2025, and FRHPe-02, which fail to correctly assess rTBI risk. This paper provides recommendations for enhancing motorcycle helmet design to improve protection against rotational traumatic brain injuries.

KEYWORDS – Helmet; Brain injury; TBI; Rotational brain injury; Biomechanics; Motorcycle crash; Concussion; Diffuse axonal injury, Subdural hematoma; Head injury; Skull fracture

INTRODUCTION

Two fundamental epidemiologic studies have been conducted into the causation of motorcycle accidents: The Hurt study [1] in North America and the MAIDS study [2] in Europe. The COST 327 Report [3], which is an extension of the MAIDS study, documents that three-quarters (75%) of all helmeted motorcyclist deaths are a result of injury to the brain. Linear forces are the primary factor in 31% of fatal head injuries, whereas rotational forces were found to be the principal cause in over 60% of cases.

While the helmet is considered the most effective means of rider protection [4], studies indicate that current motorcycle helmets are only 37-42% successful in preventing fatal injury [5,6]. By reducing peak linear forces acting on the head, it was believed that the risk of rotational brain injuries (rTBI), including cerebral concussion, diffuse axonal injury, and subdural hematoma, would also be mitigated. However, the biomechanical mechanisms of focal and rotational brain injuries are unique. Contemporary research shows that these mechanisms are poorly correlated [7,8], as verified by the current study.

Like most helmets, motorcycle helmets are modeled after ancient military headgear, the purpose of which is to protect against penetrating head injuries. All impacts possess both linear and oblique components, generating translational and tangential forces, respectively. The modern motorcycle helmet was introduced over 60 years ago [9]. Its outer shell serves as

Address correspondence to: John Lloyd, 32824 Michigan Ave, San Antonio, FL 33576 | Tel: 813-624-8986 | Email: John@DrBiomechanics.com

a second skull, diffusing impact forces over a larger surface area, while the liner, typically constructed of expanded polystyrene (EPS), compresses to reduce translational forces. However, a mechanism to mitigate tangential forces is absent in standard helmets. Since the liner fills the entire inner surface of the shell and is immobile, rotational inertia-induced tangential forces are transmitted directly to the brain.

In the United States, motorcycle helmets are certified by manufacturers to comply with Federal Motor Vehicle Safety Standard (FMVSS) #218 (also known as DOT certification) [10]. Testing includes helmeted head impacts onto flat and hazard anvils at impact speeds up to 6 m/s (13.4 mph). Motorcycle helmets are considered acceptable according to this standard if recorded peak linear accelerations do not exceed 400g, do not exceed 200g for more than 2.0 milliseconds, and do not exceed 150g for more than 4.0 milliseconds. The Snell Memorial Foundation (SMF) offers voluntary motorsport helmet standards that require higher impact protection [11]. However, current standards fail to adequately evaluate the protection afforded by motorcycle helmets against rotational brain injury (rTBI).

The updated United Nations standard (ECE 22.06) [12], which governs motorcycle helmets in Europe, recently incorporated a new method to evaluate the risk of rTBI by calculating the Brain Injury Criterion (BrIC) [13], similar to that previously published by Lloyd [14]. The Fédération Internationale de Motocyclisme (FIM), also known as the International Motorcycling Federation, is the global governing body for motorcycle racing. The new FIM helmet safety standard FRHPhe-02 [15], which will become mandatory across all FIM-related motorcycle competition from 2026 onward, will have an unrestrained oblique impact test component similar to ECE 22.06 to evaluate the risk of rTBI, as does the new Snell M2025 standard [16].

To consider whether a motorcycle helmet may reduce or prevent injuries, it is essential to understand the two primary mechanisms associated with traumatic head and brain injury – impact loading and inertial loading. A direct blow transmitted primarily through the center of mass of the head produces impact loading, which can result in focal injuries such as contusions, lacerations, and external hematomas, as well as skull fractures with coup/contrecoup brain contusions and intraparenchymal hemorrhages, which may lead to encephalomalacia [17]. Rotational movement of the brain relative to the skull induces inertial loading, which can cause diffuse brain injuries, such as cerebral concussion [18]. Inertial loading on the neural structures within the brain can produce axonal injury [19,20], often identified in living tissue by the presence of punctate hemorrhages. Whereas its effects at the brain's surface can cause subdural hemorrhage (SDH) due to bridging vein rupture [21].

Skull Fracture: Thresholds for skull fracture have been determined based on experiments involving 25 gel-filled human cadaveric skulls that were exposed to impacts [22]. Each head was filled with gelatin to represent total head mass, and the rubber skin of a Hybrid II mannequin covered the skull. A series of frontal, occipital, and temporal blows were delivered to the suspended cadaveric heads, during which linear accelerations were measured. A skull fracture threshold of 250 g was determined for frontal and occipital impacts three milliseconds or less in duration, decreasing to 140 g for impact durations greater than seven milliseconds. The skull fracture threshold for lateral impacts was reported to be 120 g over three milliseconds, decreasing to 90 g for impact durations greater than seven milliseconds. These findings indicate that skull fracture threshold and impact duration are inversely related.

Brain Injury: Research conducted by Holbourn [23] was the first to cite angular acceleration as the principal mechanism in rotational traumatic brain injury (rTBI). In studies involving live primates and physical models, Gennarelli, Thibault, and colleagues investigated the importance of rotational acceleration in brain injury causation, concluding that angular acceleration contributes more than linear acceleration to the generation of diffuse brain injuries, including concussion, subdural hematomas and axonal shear injuries [19,20,24,25,26]. Ommaya theorized that diffuse effects of the rotational components of inertial loading are produced by a centripetal progression of strains that begin at the outer surface of the brain and extend inward, with a corresponding increase in injury severity. He expressed this risk of rotational injury using a criterion based on both angular velocity and angular acceleration [27]

According to Gennarelli, the most common type of acute traumatic brain injury results from the tearing of veins that bridge the subdural space as they travel from the brain's surface to the various dural sinuses [21]. The severity of injury associated with bridging vein rupture has led to several studies of their mechanical failure properties [28,29,30,31,32,33]. Subdural hematomas and axonal injury are sensitive to the direction of impact, where SDH are more common in sagittal plane impacts, while axonal injuries tend to be associated with head impacts that generate tangential forces in the coronal plane [20]. Epidural hematomas occur due to linear forces acting on the skull and the underlying meningeal vessels but are not considered brain injuries [34].

METHODS

The following is an analysis of 498 unhelmeted vs. certified and non-certified motorcycle helmet tests at impact speeds ranging from 6 to 18 m/s (13 to 40 mph).

Test Apparatus: In accordance with prior published test methods [14,35,36] test apparatuses were constructed to evaluate the biomechanical protection against focal and rotational head and brain injuries afforded by DOT-certified and non-certified motorcycle helmets with comparison the unhelmeted condition. Impact attenuation testing of motorcycle helmets typically involves guided drop tests of an instrumented helmeted Hybrid III head and neck at impact speeds up to 8 m/s (18 mph) [10]. Many of the reported tests in this analysis were similarly performed (Figure 1).

Figure 1: Guided free-fall drop test system with Hybrid III head and neck

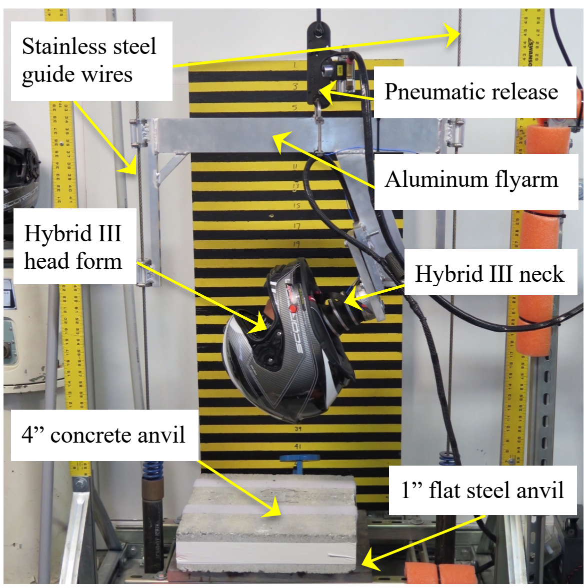

However, since impact velocity is related to the square root of the drop height ($v = \sqrt{2gh}$), where g is the acceleration due to gravity and h is the fall height, impact speeds greater than 8.5 m/s are challenging to achieve using a vertical drop test apparatus. Pendulum arms were utilized to achieve higher impact speeds. Total impact velocity is increased due to the linear and angular components of the drop height $v = \sqrt{2gh^2 + 2gr^2}$, where r is the radius of the arc subscribed by the pendulum [37].

For still higher impact velocities, twin force-balanced pendulum arms were used, which collided at a center point. The pendulum arms were simultaneously released under force from air cylinders, generating a combined impact velocity of up to 18 m/s (40 mph). A 50th percentile Hybrid III head and neck was affixed to the end of one pendulum, while an equally weighted metal anvil was attached to the other (Figure 2).

Figure 2: Twin pendulum arm impact attenuation apparatus

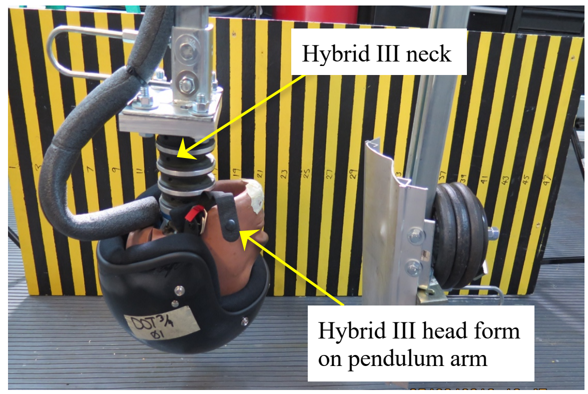

By incorporating a Hybrid III neck, the impact tests produce rotation at the axis between the head and neck, facilitating the measurement of more realistic head and brain angular kinematics. The methods presented herein are based on standardized helmet test methodologies and published research.

Helmets: Twenty-eight standard DOT-certified motorcycle helmet models were selected for testing based on popularity among motorcyclists and range of pricing, including representative models of full-coverage (full-face/modular), open-face (three-quarter), and shorty (half-helmet) styles, as shown in Figure 3 below. Two advanced DOT-certified full-face motorcycle helmet designs (6D ATS-1R and Bell DLX Qualifier) were included in this study, which incorporate technologies that allow some independent movement of the helmet shell, thereby reducing the angular kinematics that are transmitted to the head and brain. All certified helmets displayed the DOT sticker, indicating their protective performance met the FMVSS218 motorcycle helmet testing standard [10]. In addition, five novelty (non-certified) motorcycle helmet models were evaluated.

Multiple samples of each model were purchased for testing. Helmet sizes were selected based on the best fit for the Hybrid III head form, representative of a 50th percentile US adult male.

Figure 3: Motorcycle helmet models evaluated

Sensors: Four PCB Piezotronics tri-axial accelerometers (model # 356A01) were mounted in an XYZ array at the center of mass of the Hybrid III head form, along with a tri-axial angular rate sensor produced by Diversified Technical Systems, from which data was processed in accordance with the SAE coordinate system (composite Figure 4).

Figure 4: Sensor installation in Hybrid III head form

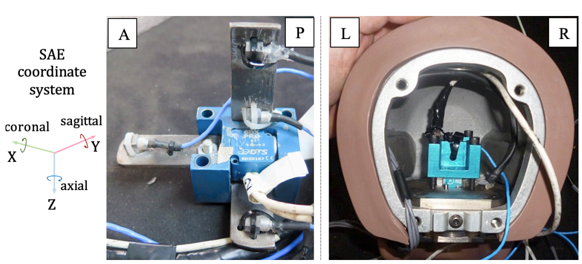

Testing: Repeated impacts of the unhelmeted head form onto a modular elastic polymer (MEP) of durometer 60 were performed at the beginning and end of each series to ensure the validity and reliability of the test method. The frontal region and occipital area on each new helmet were impacted twice, in accordance with most motorcycle helmet standards. High-speed video recordings were acquired at 2500 frames per second using an Edgertronic color high-speed video camera. In total, 93 tests were performed on an unhelmeted Hybrid III head form, 75 advanced and 121 standard DOT-certified full-face helmet tests, 56 tests on DOT-certified open-face helmets, 93 DOT-certified half-helmet tests, as well as 60 tests on novelty motorcycle helmets.

Data Acquisition and Analysis: Data from the analog sensors were acquired at 20,000 samples per second using a National Instruments compact DAQ data acquisition system and LabVIEW software (National Instruments, Austin, TX). The National Instruments compact DAQ data acquisition system includes a NI-cDAQ-9178 base, NI-9234 analog modules for the linear accelerometers, a NI-9239 module for the DTS angular rate sensor, and a NI-9481 trigger to control the high-speed camera and release mechanism. The NI cDAQ data acquisition modules have built-in anti-aliasing filters that adjust automatically based on the sampling rate. The raw data was filtered in Matlab™ (The MathWorks, Natick, MA) using a phaseless eighth-order Butterworth filter with cutoff frequencies of 1650 Hz (CFC 1000) and 300Hz (CFC 180) for the linear accelerometers and angular rate sensors, respectively, per SAE J211 [38]. Angular acceleration values for the sagittal, coronal, and axial planes were computed from angular velocity data using the central difference by least squares method (Equation 1):

Equation 1: Central difference by least squares method

$$f(x_n) = (f(x_n + 2) + 8fx_n - 8f(x_n + 1) - fx_n - 2)/12dx$$

For comparison, angular acceleration values were also derived from the array of linear accelerometers using the mathematical method proffered by Padgaonkar *et al.* [39].

Linear velocity at the moment of impact was calculated by integrating linear acceleration, while linear and angular jerk were computed by differentiating linear and angular acceleration components. Derived values were filtered as above using a cutoff frequency of 500 Hz, established based on Fast Fourier Transform analysis. Mathematical methods were performed using Matlab™ to compute characteristic values from variables of interest. Figure 5 below illustrates linear acceleration, angular velocity, and angular acceleration graphs associated with a standard DOT-certified helmeted head impact.

Figure 5: Typical linear acceleration, angular velocity, and angular acceleration plots

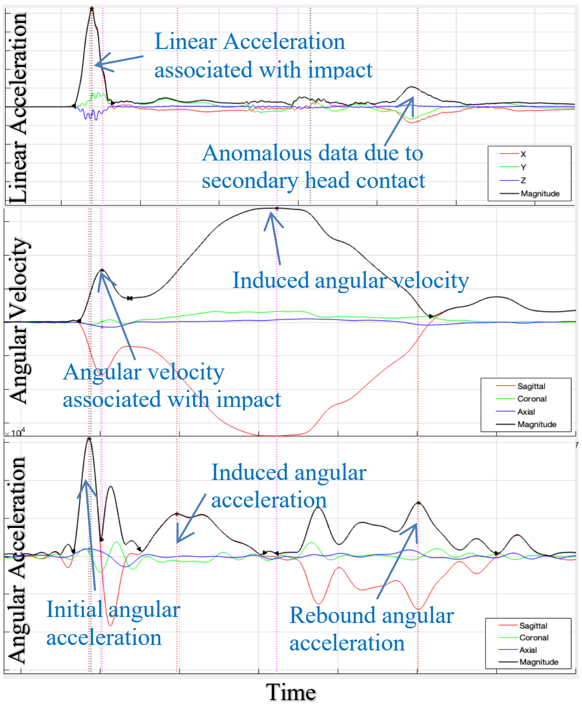

Linear Acceleration

Impact duration was determined, adapted from the method by Depreitere [33], based on the resultant linear acceleration signal, where impact start (LAIS) is the time at which the pre-peak resultant linear acceleration exceeds 3 g, and impact end (LAIE) is the time at which the principal component of linear acceleration crosses the x-axis. (Figure 6). The gradient from impulse start point to peak was computed, as was the area under the resultant linear acceleration curve from start to endpoints.

Figure 6: Metrics calculated based on linear acceleration data

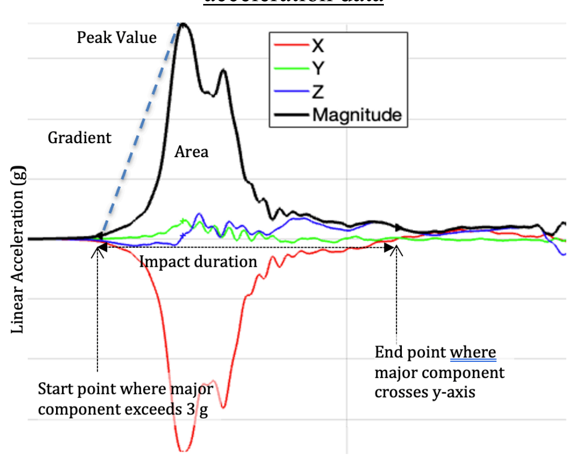

LVM	MeanLAM	LA_duration	Time_LA400
LAX	LJX	LA_area	GSI
LAY	LJY	LA_gradient	HIC15
LAZ	LJZ	Time_LA150	SFC
LAM	LJM	Time_LA200	Max_Pressure

Linear acceleration values were used to calculate Maximum Pressure [13] (Equation 2), Gadd Severity Index (GSI) [40] (Equation 3), and Head Injury Criterion (HIC_{15}) [41] (Equation 4).

Equation 2: Maximum Pressure [13]

$$Max\ pressure = a_{max}\ x\ 0.9$$

Equation 3: Gadd Severity Index [40]

$$GSI = \int_0^t a^{2.5}.dt$$

The Head Injury Criterion (HIC) is an empirical measure of impact severity describing the relationship between the linear acceleration magnitude and impact duration (Equation 4).

Equation 4: Head Injury Criterion [41]

$$HIC_{15} = max\left\{\left[\frac{1}{t_2 - t_1}\int_{t_a}^{t_2} a(t)dt\right]^{2.5} (t_2 - t_1)\right\}$$

where a is resultant head acceleration, t_2-t_1 ≤ 15 msec

HIC value is used to predict the risk of focal head and brain injury (Figure 7), with the following definitions:

Minor – skull trauma without loss of consciousness; nose fracture; superficial injuries

Moderate – skull trauma with or without dislocated skull fracture and brief loss of consciousness. Fracture of facial bones without dislocation; deep wound(s)

Critical – Cerebral contusion, loss of consciousness for more than 12 hours with intracranial hemorrhaging and other neurological signs; recovery uncertain.

Figure 7: Probability of specific head trauma level based on HIC value [42]

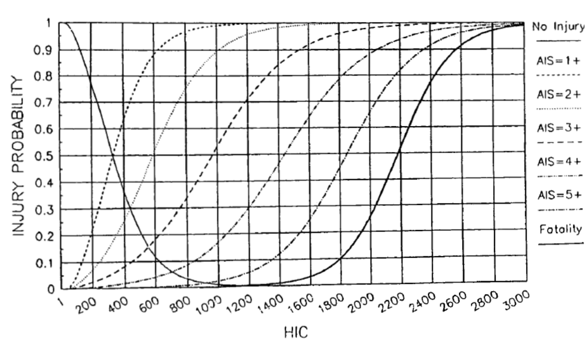

Angular Velocity

The initial impact-related peak angular velocity (AVM1) was determined as the maximum resultant angular velocity associated with peak linear acceleration (LAM), with a start time point (AVIS1) when the principal component exceeds one rad/s and the end time point (AVIE1) where the primary component crosses below the x-axis after AVM1, or the lowest resultant angular velocity value between the initial and induced angular velocity peaks (AVM1, AVM2). Similarly, the start time point (AVIS2) for the induced angular velocity was determined where the principal component of AVM2 exceeds one rad/s before AVM2 peak but after AVIE1, and the end time point (AVIE2) where the primary component crosses below the x-axis after AVM2. Component values (coronal, sagittal, axial) are reported at AVM1 and AVM2 peaks. The gradients from the start time point to the peak resultant angular velocity were computed and the areas under the resultant curves were calculated between their respective start and end time points. Mean angular velocity was calculated from the start time point of the first resultant angular velocity peak to the end time point of the induced angular velocity peak (Figure 8). It was notes that the induced angular velocity of the impacted head form was considerably greater than the impact-related angular velocity.

Figure 8: Metrics calculated based on angular velocity data

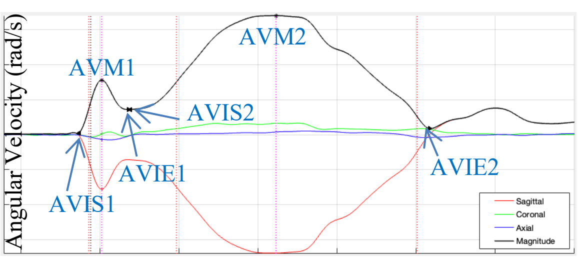

ADC	AVS2	AVM1b_area	AVM_Durat	AIS3_AVM1
ADS	AVA2	AVM1_grad	MPS_AVM1	AIS4_AVM1
ADA	AVM2	AVM2_area	MPS_AVM2	AIS5_AVM1
MaxADM	MeanAVC	AVM2a_area	CDSM_AVM1	AIS1_AVM2
AVC1	MeanAVS	AVM2b_area	CDSM_AVM2	AIS2_AVM2
AVS1	MeanAVA	AVM2_grad	BrIC_AVM1	AIS3_AVM2
AVA1	MeanAVM	AVMpos_area	BrIC_AVM2	AIS4_AVM2
AVM1	AVM1_area	AVMneg_area	AIS1_AVM1	AIS5_AVM2
AVC2	AVM1a_area	AVM_Tot_Area	AIS2_AVM1	

Angular velocity values were also used to derive Global Maximum Principal Strain (MPS) [13] (Equation 5), Cumulative Strain Damage Measure (CSDM) [13,43] (Equation 6), and Brain Injury Criterion (BrIC) [13] (Equation 7).

Equation 5: Maximum Principal Strain [13]

$$MPS = -peak\ angular\ velocity\ magnitude * 0.01$$

Equation 6: Cumulative Strain Damage Measure [13, 43]

$$CSDM = -(peak\ angular\ velocity\ magnitude * 0.01) - 0.30$$

An analysis method validated by Takhounts [13] establishes physical injury criteria for various rotational traumatic brain injuries. It uses anthropomorphic test device (ATD) data to calculate a kinematically based brain injury criterion (BrIC) for Hybrid III head and neck impact testing. This method is utilized to express the risk of rTBI according to the 2008 Abbreviated Injury Scale from the Association for the Advancement of Automotive Medicine [44] in terms of peak head angular velocity components, where:

Equation 7: Brain Injury Criterion [13]

$$BrIC = \sqrt{(AV_{coronal}/66.25)^2 + (AV_{sagittal}/56.45)^2 + (AV_{axial}/42.87)^2}$$

The probability of brain injury for AIS 1-5 was thus computed as a function of BrIC [13], and represented graphically in Figure 9, along with validation data from NFL AIS1-2 cases [45]:

		AIS	Description
$P(AIS)$	0.065	1	Mild TBI / concussion
$= 1 - e^{-\left(\frac{BrIC-0.523}{n}\right)^{1.8}}$	0.324	2	Severe concussion
	0.531	3	Serious brain injury
Where the value for n is substituted according to the table alongside:	0.647	4	Severe brain injury
	0.673	5	Critical brain injury
		6	Fatal injury

Figure 9: Brain Injury Risk Curves

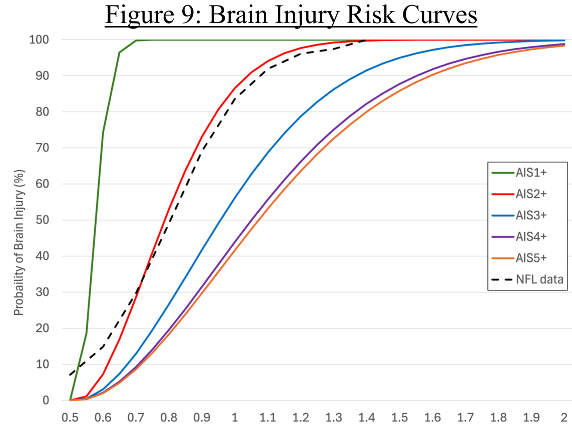

Angular Acceleration

Impact-related peak angular acceleration (AAM1) was determined as the maximum angular acceleration value associated with peak linear acceleration (LAM), with a start time point (AAIS1) where the principal component exceeded five percent of peak AAM1 and the end time point (AAIE1) where the primary component crossed below the x-axis after AAM1. Similarly, induced peak angular acceleration (AAM2) was determined as the maximum angular acceleration value between the start time point for AVM2 and the induced peak angular velocity (AVM2), with start time point (AAIS2) where the principal component exceeded five percent of peak AAM2 and the end time point (AAIE2) where the primary component crossed below the x-axis after AAM2. Finally, rebound peak angular acceleration (AAM3) was determined as the maximum value between peak AVM2 and the end time point for the resultant induced angular velocity peak (AVIE2). To avoid any effect due to a secondary erroneous linear acceleration peak (LAM2), if such were present, AAM3 was determined as the maximum resultant angular acceleration value between peak AVM2 and 1.5 milliseconds prior to LAM2. The start time point for AAM3 (AAIS3) was computed where the principal component again exceeded five percent of peak AAM3, and the end time point (AAIE3) where the primary component crossed below the x-axis after AAM3. Gradients and areas for the three resultant angular acceleration peaks and the mean resultant angular acceleration from AAIS1 to AAIE3 were calculated as described above. Additionally, the total area for the sum of positive head accelerations (AAM1 and AAM2) was computed along with the total area for the negative head acceleration (AAIM3) based on the sign of the primary component (Figure 10).

Figure 10: Metrics calculated based on angular acceleration data

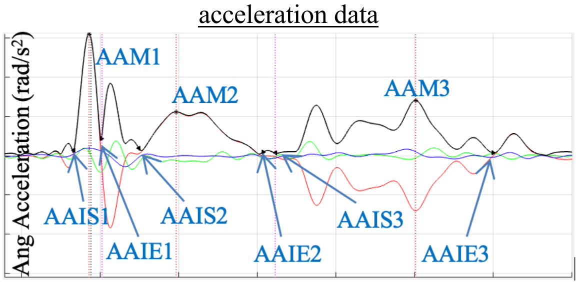

AAC1	MeanAAM2	MeanAAM	AAM1a_area	AAM3_area
AAS1	AAC3	NineAAMax	AAM1b_area	AAM3a_area
AAA1	AAS3	AJC	AAM1_grad	AAM3b_area
AAM1	AAA3	AJS	AAM2_durat	AAM3_grad
MeanAAM1	AAM3	AJA	AAM2_area	AAMpos_area
AAC2	MeanAAM3	AJM	AAM2a_area	AAMneg_area
AAS2	MeanAAC	MeanAJM	AAM2b_area	AAM_Tot_Area
AAA2	MeanAAS	AAM1_durat	AAM2_grad	AAM_Duration
AAM2	MeanAAA	AAM1_area	AAM3_durat	

Means and standard deviations were calculated across repeated tests for each helmet model. If more than 10 of the computed variables were outside of two standard deviations of the mean ($\mu \pm 2SD$), those tests were omitted from further analysis. The following results are, therefore, based on 444 impact tests, including 80 unhelmeted impact tests, 65 advanced and 113 standard DOT full-face helmet tests, 49 DOT open-face helmet tests, 84 DOT half-helmet tests, and 53 novelty helmet tests.

RESULTS

Tables 1-9, which summarize key results, are presented in the Appendix.

Figures 11 through 13, below, present a comparison of results for unhelmeted, advanced DOT, standard DOT, and novelty helmet impact tests. Figure 11 illustrates linear acceleration responses, showing that the unhelmeted and novelty helmet conditions produce higher peak magnitudes over substantially shorter impact durations compared to the advanced and standard DOT-certified helmets.

Figure 11: Comparison of linear acceleration results for unhelmeted and helmeted impacts

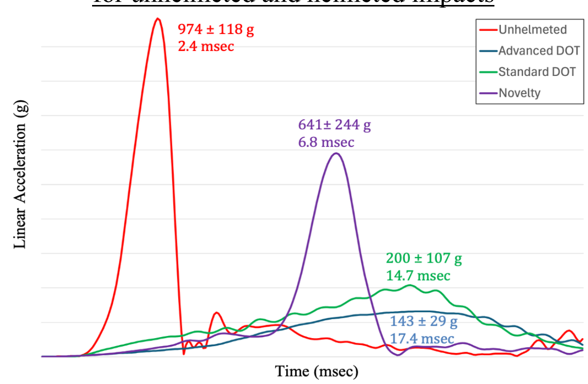

Across all DOT helmet tests, the induced angular velocity (AVM2) was more than double the initial peak angular velocity (AVM1) (Tables 4-5 and Figure 12). Other studies have only reported impact-related angular velocity values, thereby inaccurately presenting the protective performance of DOT-certified motorcycle helmets.

The total impact duration associated with angular velocity was 50 percent greater for DOT helmets compared to the unhelmeted condition. However, the total areas under the angular velocity curves were similar. This finding suggests that the total energy associated with rotational kinematics acting on the brain is similar for the helmeted and unhelmeted conditions, indicating that standard DOT-certified motorcycle helmets do not mitigate rotational inertia related to head impacts.

Figure 12: Comparison of angular velocity results for unhelmeted and helmeted impacts

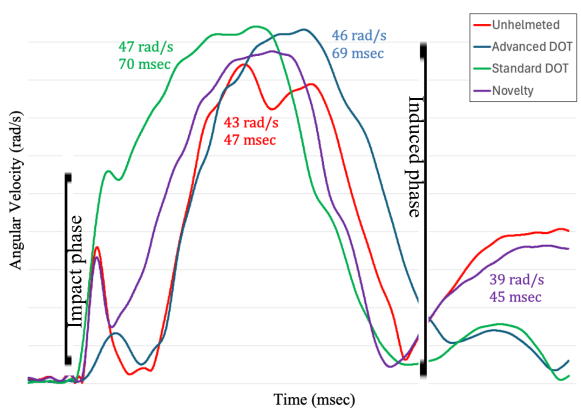

Similar to the linear acceleration results, the duration over which forces associated with angular acceleration are exerted on the brain is significantly less across unhelmeted and novelty helmet tests, compared to the advanced and standard DOT helmets (Figure 13).

Figure 13: Comparison of angular acceleration results for unhelmeted and helmeted impacts

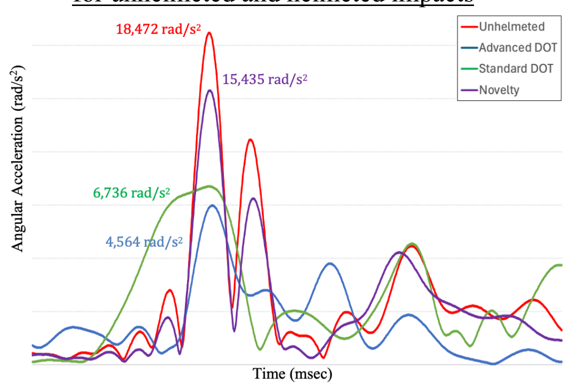

Further analysis of the results illustrates the following specific findings:

Skull Fracture

Peak linear acceleration was substantially reduced across DOT-certified helmeted impacts by approximately 81% compared to the unhelmeted condition. Impact duration associated with DOT helmeted head impacts averaged 12 to 17 msec, whereas mean unhelmeted head impact duration was 2.4 msec.

Research by Ono [22] reports that the thresholds for skull fracture for frontal impacts and lateral impacts of duration longer than seven milliseconds are 140 g and 90 g, respectively. The results presented in Figure 14 indicate that while the advanced DOT helmets performed best, none of the helmets tested provide adequate protection against both frontal/occipital and lateral skull fractures. Novelty helmets provide, on average, only a 34% reduction in the risk of skull fracture compared to the unhelmeted condition.

Figure 14: Motorcycle Helmet Protection against Skull Fracture

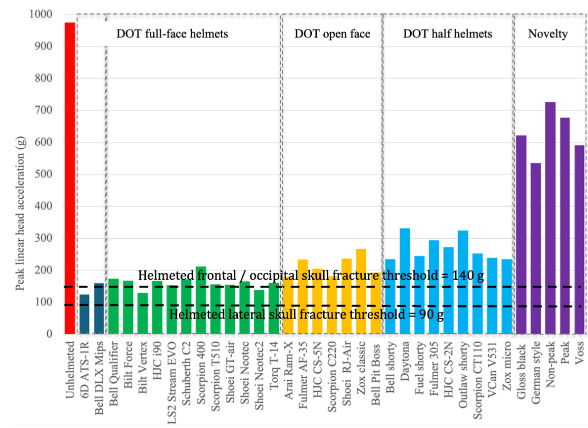

Legend: Unhelmeted (red)
Advanced DOT-full face (dark blue)
Novelty (purple)
Standard DOT - Full face (green)
Standard DOT - Open face (orange)
Standard DOT – Half-helmet (light blue)

Focal Head and Brain Injury

The Head Injury Criterion (HIC) is an empirical measure of impact severity that describes the relationship between the linear acceleration magnitude, duration of impact, and the risk of focal head and brain injury. HIC is often used to predict the risk of focal head and brain trauma.

The computed HIC values for each of the tested DOT-certified helmets are substantially less than that for the unhelmeted condition, whereas the novelty helmets did not perform as effectively (Figure 15).

Figure 15: Head Injury Criterion (HIC)

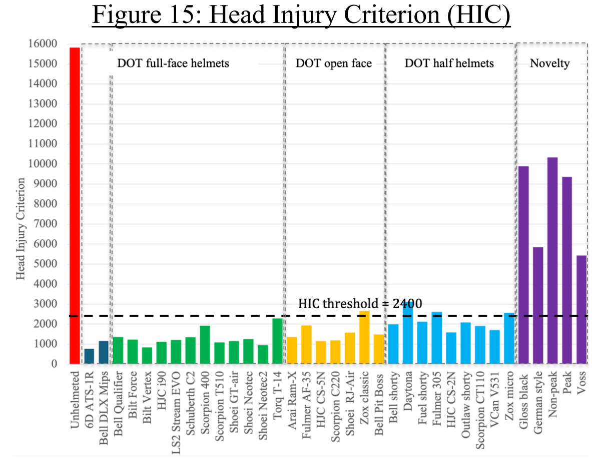

Figure 16 indicates that the use of a DOT-certified motorcycle helmet reduces the HIC value by approximately 92 percent compared to the unhelmeted condition, thereby substantially mitigating the risk of extracranial focal injuries, such as contusions, lacerations, and external hematomas, as well as skull fractures and focal brain injuries. However, standard DOT helmets still present a significant risk of focal head and brain injury, compared to the Advanced DOT helmets. Novelty motorcycle helmets offer inadequate protection against such injuries. HIC value was not influenced significantly by impact velocity. Thus, helmets can provide protection against focal brain injuries at higher impact speeds.

Figure 16: Probability of focal head and brain trauma based on HIC value (42)

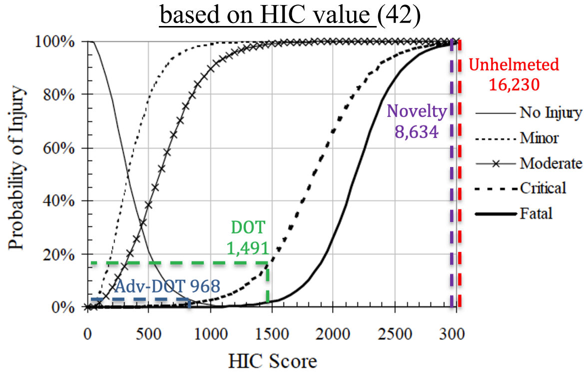

Rotational Brain Injury

Consistent with human anatomy, any motion of the Hybrid III head and neck during the immediate post-impact phase is constrained by the head-neck interface. The FRHPhe-02 standard includes a measure of peak angular acceleration, the prescribed limit of 10,000 radians per second squared, which was met by most of the tested DOT helmets (Figure 17).

Figure 17: Motorcycle helmet protection against Peak Angular Acceleration

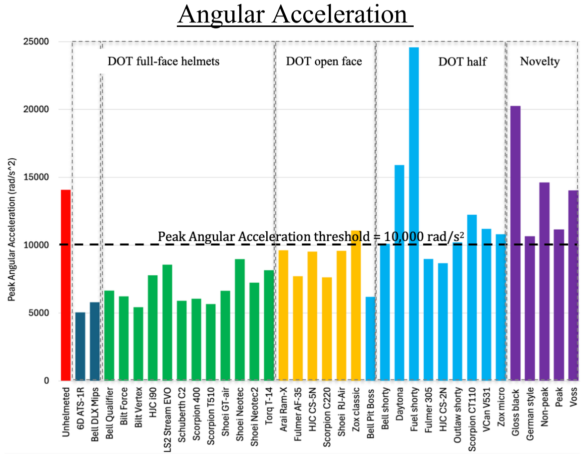

Helmets decrease peak forces associated with impact-related linear head acceleration by extending the duration over which the impact is experienced. The average impact duration involving a DOT-certified motorcycle helmet is between 12 and 17 milliseconds. Figure 18, below, on which the helmeted impact test results are plot against thresholds proffered by Löwenhielm [28,29,30] and Depreitere [33], indicates that all DOT-certified motorcycle helmets fail to provide adequate protection to prevent subdural hematomas at real-world crash speeds. Interestingly, results for the unhelmeted condition and one novelty helmet do not exceed the biomechanical threshold for this critical AIS-5 rotational brain injury due to the significantly shorter impact duration.

Figure 18: Motorcycle Helmet Protection against Rotational Brain Injury (after Depreitere, 2006)

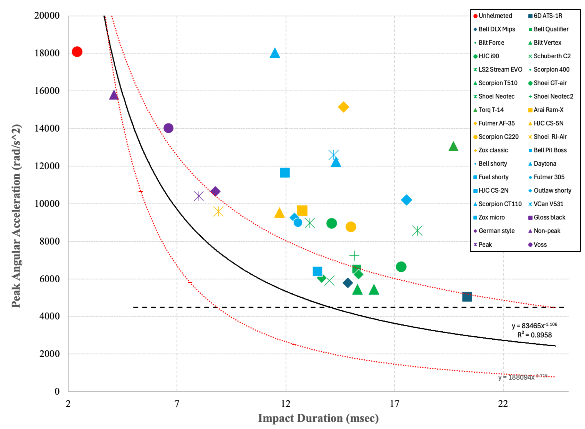

The new ECE 22.06 European helmet standard [12], the Snell M2025 standard [16], and the anticipated FIM FRHPhe-02 competition standard [15] incorporate the Brain Injury Criterion (BrIC) [13] to evaluate the risk of rotational brain injuries associated with motorcycle helmet impacts. The stated acceptable BrIC value in these standards is 0.78, which equates to an AIS-5 rTBI of 16%.

It is interesting to note that all the novelty helmet models tested met this threshold and seemingly performed better than all but one of the DOT-certified helmets (Figure 19 and Tables 7-8). The novelty helmet designs generated the lowest risk of AIS 3 to 5 for moderate-to-critical rotational brain injuries (rTBI), even outperforming the best advanced DOT helmets, likely due to their smaller size and lower mass, which induces less rotational inertia.

Figure 19: Brain Injury Criterion (BrIC)

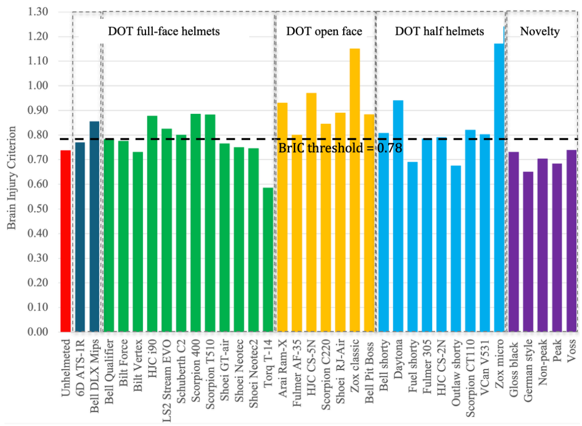

While overall peak angular acceleration was higher for the unhelmeted condition when considered in conjunction with impact duration, it was discovered that standard DOT-certified helmets present a substantially increased risk of rotational brain injury. Standard motorcycle helmets increase the risk of AIS 2 to 5 rotational brain injuries, on average, by about 30 percent compared to the unprotected condition. Whereas, advanced helmets performed, on average, about 5 percent better than standard certified helmets.

DISCUSSION

Lessons Learned about Helmet Testing

One of the more significant findings of this study is that the induced angular velocity of the impacted head is substantially greater than the impact-related angular velocity (Figures 8 and 12, as well as Tables 3-9). This demonstrates that the rebound effect is profoundly more critical to the risk of rotational brain injury than the angular velocity generated by the initial impact. Peak angular velocity will be grossly underestimated if the induced response is not quantified. Consequently, any measure of BrIC or risk of AIS 2 through 5 rTBI will be miscalculated.

The ECE 22.06 European helmet standard [12], the anticipated FIM FRHPhe-02 race standard [15], and the Snell M2025 standard [16] present a substantial advancement in addressing the risks of rotational brain injury through oblique impact testing. However, a critical methodological deficiency of these tests has been identified within the scope of this study.

The standardized oblique impact tests involve controlled impacts in which the helmeted head form is positioned in a cradle, which guides the falling head onto a rigid, flat surface tilted at 45 degrees (composite Figure 20). In the new tests, the cradle and guidance system do not influence the motion of the head form from the instant the helmet contacts the anvil surface.

Composite Figure 20: Oblique Impact Test for rTBI

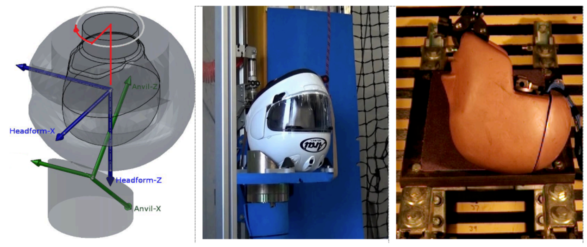

Testing consistent with this methodology was undertaken to evaluate how results might be affected (Figure 20c).

As illustrated in Figure 21, the absence of a neck during the oblique helmet testing permits unrestrained post-impact motion of the head form. Since oblique impact testing required by the above-listed motorcycle helmet standards is unrestrained by a surrogate neck, the methods do not correctly capture induced angular velocity and fail to properly quantify BrIC and the associated risk of rotational traumatic brain injuries.

Figure 21: Angular velocity comparison between unrestrained and restrained oblique test

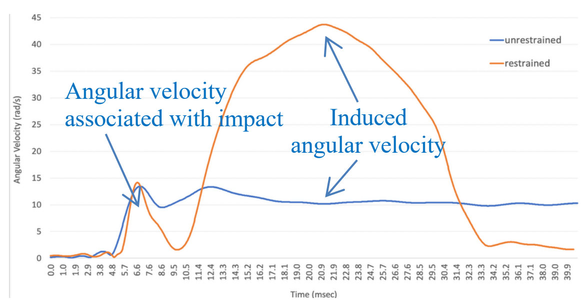

Moreover, the absence of the Hybrid III neck in the ECE 22.06 [12], FRHPhe-02 [15], and the Snell M2025 [16] standards is inconsistent with the ATD testing methodology for calculating Brain Injury Criterion, as prescribed by Takhounts [13].

Thus, anchoring the head form to a surrogate neck is critical to accurately quantifying and understanding the induced angular head and brain kinematics generated in real-world crashes, which are the underlying mechanical etiology of rotational traumatic brain injuries. Additional findings of this study demonstrate that the orientation of the neck is irrelevant since peak linear and rotational kinematics precede any motion of the Hybrid III neck. Hence, the Hybrid III head and neck can be rotated on a guided free-fall drop test apparatus to meet the oblique impact testing requirements.

The important measures for the biomechanical evaluation of helmet performance against focal and rotational head and brain injuries, based on this study, are the Head Injury Criterion (HIC) and Brain Injury Criterion (BrIC), respectively. All other variables, including peak linear acceleration, impact duration and dwell time, skull fracture criterion, peak angular velocity, and peak angular acceleration, are incorporated by and highly correlated with the derivative variables of HIC and BrIC.

The current acceptable HIC value, under ECE 22.06 [12], is 2400. It is proposed that motorcycle helmet standards adopt a maximum HIC value of 1000, in accordance with accepted automobile standards [46], thereby minimizing the risk of focal head and brain injuries. A maximum acceptable BrIC value of 0.72 is recommended, which would reduce the risk of AIS-5 critical rotational brain injury to 10%.

Though the results presented in this study indicate that novelty helmets afford the lowest risk of moderate-to-critical rotational brain injuries in helmeted head impacts, the protection afforded against focal head and brain injuries by this category of helmets is no more effective than the unhelmeted condition. It is imperative that any helmet suitable for motorcycling, or any other activity in which there is a risk of head trauma, offer protection against both focal and rotational injuries, based on the thresholds proposed above.

Helmet Design Recommendations

Helmeted skull fracture thresholds are lowest in lateral impacts (Figure 14). It is suggested therefore that helmet shells be strengthened in the temporal and parietal regions, perhaps using stronger materials such as carbon fiber, thereby distributing forces over a larger surface area and reducing peak accelerations below injury thresholds.

While HIC values were similar between frontal and occipital tests for the DOT-certified helmets, calculated BrIC values were significantly lower across frontal helmet impact tests (Tables 1-2 and 7-8). It was observed during the frontal impact tests, based on high-speed videos, that the front edge of the helmet would contact and drag across the surface. Additional testing was conducted to evaluate the effect of surface coefficient of friction on rTBI risk by performing repeated impact tests onto different surfaces, including concrete, flat steel, sandpaper (80-grit), High-Density Polyethylene (HDPE), and Teflon. A strong negative association was discovered between the surface coefficient of friction and Brain Injury Criterion / rTBI risk. A 38% difference in computed BrIC values was found between the low and high coefficient of friction surfaces, where more slippery surfaces induce more rapid helmet rotation, thereby generating higher induced peak angular velocity and, consequently, higher BrIC values (Figure 22).

Figure 22: Angular velocity induced by the surface coefficient of friction

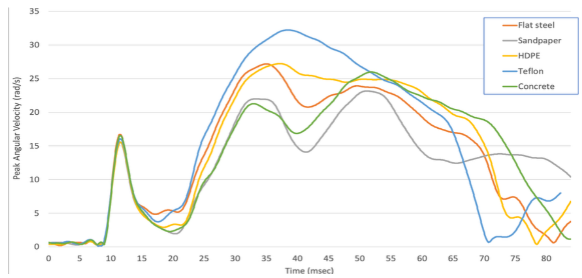

It is surmised that the difference between the coefficient of friction at the impact surface and head-liner interface generates shear forces. Advanced helmet technologies, such as MiPS (multi-directional impact system) and the omnidirectional suspension system, help mitigate this effect by decoupling the helmet from the head. Based on this finding, it is suggested that rotational forces could be significantly reduced by matching the drag factor between the impact surface and that at the head-liner interface.

Lastly, based on the principles of physics, it is suggested that if the mass of the helmet is distributed such that the center of mass of the head is relatively unaffected by the addition of a helmet, then, perhaps, the increased rotational inertia acting on the brain would be more natural. This finding is reflected in the results for the DOT-certified open-face helmets, in which a greater risk of rTBI was observed compared to the full-face and half-helmet designs, believed to be due to the incongruity between the head form and helmeted center of mass, of which further analysis is warranted.

There is valuable information to be learned from the results of the novelty helmet tests, which appear to present enhanced protection against rotational brain injuries, though failing to afford adequate protection against potentially lethal focal injuries. Current motorcycle helmet designs may be oversized to reduce translational forces, resulting in larger and heavier helmets, thereby generating greater rotational inertia and hence increasing the rTBI risk. Rotational brain injuries are now the primary cause of fatality in two-thirds of helmeted motorcycle crashes since linear forces are well mitigated by certified helmets. Protection against focal injuries is paramount, but it also needs to be balanced against the increased risk of rotational brain injuries. Manufacturers should evaluate materials that allow the development of smaller and lighter helmets.

In summary, more effective motorcycle helmet designs should be explored, along with analyzing the effects of weight, size, helmeted head center of mass, and helmet-to-surface drag factor on kinematic and tissue-based metrics.

Limitations and Future Work

Brain Injury Criterion (BrIC) and its associated injury risk functions (AIS 1-5) were computed and reported within this paper since it is the metric chosen by ECE 22.06, Snell 2025, and FRHPhe-02 standards to quantify the risk of brain injury associated with helmeted head impacts in motorcycling. It is recognized that BrIC tends to over-estimate the risk of severe-to-fatal (AIS4+) brain injuries [47] likely due to the Eppinger mass-ratio scale factor [48], which is not supported by more recent finite element analyses due to lack of geometrical similitude [49]. Despite this limitation, the reported BrIC and AIS 1-5 brain injury risk values are useful comparative measures when relating the protective performance of different motorcycle helmets.

Since the BrIC metric is based solely on angular velocity, it may not be the most robust method for assessing the risk of rotational brain injury. Dr. Gabler and his team have formulated a new series of metrics, including UBrIC (Universal Brain Injury Criterion) [50], and the more recent DAMAGE (Diffuse Axonal Multi-Axis General Evaluation) [51] metric, which is computed based on both angular velocity and angular acceleration measures. Their methods follow an approach proposed by Ommaya forty years ago that a brain injury criterion should consider both rotational kinematic variables [27]. Ommaya proposed two rotational injury scales, the first for events associated with relatively slow angular velocities ($\dot{\theta}$< 30 rad/s) and the second for events associated with higher angular velocities ($\dot{\theta} \geq 30$ rad/s). Based on the work presented herein, and with reference to Tables 3 through 9, it appears that a peak angular velocity of 30 radians per second is consistent with a 50 percent risk of AIS2 rotational brain injury, increasing to 90% risk of AIS2 rTBI for impacts producing a peak angular velocity of 50 rad/s. Of the nearly 500 impact tests performed in this series, only a small percentage (all novelty / non DOT-certified helmet tests) generated a peak angular velocity less than 30 radians per second, in which it was observed that the risk of AIS2 rTBI was substantially reduced. These findings are consistent with Ommaya's division of a criterion between two scales. The effect of angular acceleration cannot be assessed in this paper, since quantification of rTBI risk was computed herein independent of rotational acceleration characteristics.

Brain Injury Criterion (BrIC) was chosen as the principal metric for this paper because of its adoption by ECE, Snell and FIM standards. Future work will involve expanding the analysis of this extensive dataset of motorcycle helmet impact tests to compute other kinematic-based metrics, such as HIP (Head Impact Power) [52], PRHIC (Power Rotational Injury Criterion) [53], RIC (Rotational Injury Criterion) [53], RVCI (Rotational Velocity Change Index) [54], CIBIC (Convolution of Impulse response for Brain Injury Criterion) [55], UBRIC [50] and DAMAGE [51] against finite-element computed tissue-based metrics to determine the most appropriate laboratory test method for evaluating helmet performance. The effect of the helmeted center of mass could also be further explored in subsequent analyses. It is hoped that this ongoing work will help to inform the adoption of more suitable metrics for motorcycle helmet standards and other helmet standards in the future.

An analysis is also in process, comparing helmets intended for various activities, including motorcycling, skiing, bicycle, off-road, American football, ice hockey, and military. Preliminary results suggest that helmets intended for other sports activities may outperform motorcycle helmets at similar impact speeds in terms of protection against both focal head injuries and rotational brain injuries.

CONCLUSIONS

Mandatory motorcycle helmet standards in the United States only evaluate helmet performance up to impact speeds of 13.4 miles per hour, and helmets can pass without providing adequate protection against skull fractures at this relatively low impact speed. The included analysis shows that standard DOT-certified helmets tested fail to provide adequate protection against skull fractures or rotational brain injuries associated with real-world motorcycle crashes.

The revised ECE 22.06 European standard has reintroduced oblique impact testing for computing Brain Injury Criterion (BrIC) as a measure of rotational traumatic brain injury (rTBI) risk, as recommended by the COST 327 report [3]. The voluntary Snell M2025 and forthcoming FIM FRHPhe-02 race standards have adopted an identical methodology for quantifying rTBI risk. However, the oblique impact test methods underlying these standards incorporate a critical deficiency in that induced angular velocity of the helmeted head form is not quantified due to the unrestrained helmeted head. This is not a scientifically valid approach for calculating the risk of rotational brain injuries.

Ultimately, results show that standard DOT-certified helmets afford substantial protection against focal head and brain injuries but not rotational brain injuries. Motorcycle helmets that meet the new ECE 22.06 standard appear to offer better overall protection, though the results from the current oblique testing method are questionable. Conversely, novelty helmets seem to provide better against rotational brain injuries but fail to prevent focal head and brain trauma. Emerging advanced DOT helmets that offer both focal and rotational injury mitigation are currently only available in full-face designs, and as such may not be suitable for all riders. Manufacturers may soon provide technologies to help mitigate the risk of rotational brain injuries in open-face and half-helmet designs.

Motorcyclists believe helmets are designed to protect the entire head, including the brain. Results of this and other studies show that certified helmets provide excellent protection against focal head and brain injuries, which are the leading cause of severe and fatal trauma in unhelmeted impacts, as exemplified by increased fatality rates in states that have rescinded motorcycle helmet laws. Novelty (non-certified) helmets offer inadequate focal injury protection. The defense afforded against rotational brain injuries varies between helmet models, the technology for which is constantly improving. Motorcyclists are encouraged to wear advanced certified helmets, which offer the best current protection against both focal head and rotational brain injuries.

ACKNOWLEDGMENTS

This study was funded by BRAINS, Inc.

REFERENCES

1. Hurt HH, Ouellet JV & Thom DR (1981) Motorcycle Accident Cause Factors and Identification of Countermeasures. Volume 1: Technical Report. Traffic Safety Center, University of Southern California Traffic Safety Center, Los Angeles, CA. https://rosap.ntl.bts.gov/view/dot/6450

2. ACEM (2009) MAIDS (Motorcycle Accidents In Depth Study): In-depth investigations of accidents involving powered two wheelers – Final Report 2.0. European Association of Motorcycle Manufacturers. https://www.maids-study.eu/pdf/MAIDS2.pdf

3. Chinn B, Canaple B, Derler S, Doyle D, Otte D, et al. (2001) Cost 327, Motorcycle Safety Helmets, Final report of the action. European Commission, Directorate General for Energy and Transport, Belgium.

4. Chang L, Chang G, Huang J, Huang S, Liu D et al. (2003) Finite Element Analysis of the effect of motorcycle helmet materials against impact velocity. Journal of the Chinese Institute of Engineers. 26: 835–843.

5. National Highway Transportation Safety Administration (2008) Traffic Safety Facts, Data: Motorcycles. DOT HS 811 159. National Highway Traffic Safety Administration, Washington, DC.

6. Liu B, Ivers R, Norton R, Boufous S, Blows S, Lo SK (2008) Helmets for preventing injury in motorcycle riders. Cochrane Database Syst Rev. Jan 23; (1): CD004333.

7. King AI, Yang KH, Zhang L, Hardy W, Viano DC. (2003). Is head injury caused by linear or angular acceleration; Lisbon, Portugal: IRCOBI.

8. Roy R (2007) Evaluation of Head Linear and Rotational Acceleration Response to Various Linear-Induced Impact Scenarios. Master’s Thesis, University of Tennessee.

9. Roth H. and Lombard C (1953) Crash helmet. US patent 2,625,683.

10. U.S. Department of Transportation (2013) Federal Motor Carrier Safety Administration Standard No. 218, Motorcycle helmets. Washington, DC.

11. Snell Memorial Foundation. (2019). Standard for Protective Headgear for use with Motorcycles and Other Motorized Vehicles. M2020.

12. United Nations (2021). Uniform Provisions Concerning the Approval of: Protective Helmets, of their Visors and of their Accessories for Drivers and Passengers of Motorcycles and Mopeds. Regulation No. 22-06

13. Takhounts EG, Craig MJ, Moorhouse K, McFadden J. (2013). Development of Brain Injury Criteria (BrIC). *Stapp Car Crash Journal* 57: 243-266.

14. Lloyd J. (2017). Biomechanical Evaluation of Motorcycle Helmets: Protection Against Head

and Brain Injuries. *Journal of Forensic Biomechanics. 8:3.*

15 Fédération Internationale de Motocyclisme. (2022) FIM Racing Homologatged helmet program - FRHPhe-02. Switzerland.

16 Snell Memorial Foundation. (2024). Standard for Protective Headgear for use with Motorcycles and Other Motorized Vehicles. M2025

17 Andriessen T, Jacobs B & Vos P. (2010). Clinical characteristics and pathophysiological mechanisms of focal and diffuse traumatic brain injury. J Cell Mol Med 14:10, 2381-2392

18 Gennarelli TA, Thibault LE & Ommaya AK. (1972). Pathophysiologic Responses to Rotational and Translational Accelerations of the Head. SAE Technical Paper 720970

19 Gennarelli TA, Thibault LE, Adams JH, Graham DI, Thompson CJ, Marcincin RP (1982). Diffuse axonal injury and traumatic coma in the primate. *Ann Neurol.* 12(6):564-74

20 Margulies SS and Thibault LE. (1992). A proposed tolerance criterion for diffuse axonal injury in man. *J Biomechanics* 25 (8), 917-923

21 Gennarelli T. and Thibault L (1982). Biomechanics of Acute Subdural Hematoma, *J Trauma*. 22(8), 680-686

22 Ono K. (1998). Human head impact tolerance. In Yoganandan (Ed). Frontiers in Head and Neck Trauma: Clinical and Biomechanical. *IOS Press*, Amsterdam

23 Holbourn AHS. (1943). Mechanics of Head Injuries. *The Lancet*. 242(6267):438-441

24 Gennarelli TA, Ommaya AK, Thibault LE. (1971). Comparison of translational and rotational head motions in experimental cerebral concussion. Stapp Car Crash Conference. Fifteenth Proceedings, *SAE Technical Paper* P-39, 797-803

25 Gennarelli TA, Adams JH, Graham DI. (1981). Acceleration induced head injury in the monkey I: The model, its mechanistic and physiological correlates. *Acta Neuropathol. Suppl*. 7:23-25

26 Thibault LE & Gennarelli TA. (1985). Biomechanics of diffuse brain injuries. Stapp Car Crash Conference. Twenty-Nine Proceedings, *SAE Technical Paper* 856022

27 Ommaya AK. (1985). Biomechanics of head injury: Experimental aspects. In The Biomechanics of Trauma (edited by A.M. Nahum and J.W. Melvin), pp. 245-279. Appleton-Century-Crofts, Norwalk.

28 Löwenhielm P. (1974). Dynamic properties of the parasagittal bridging veins. *Z. Reehtsmedizin.* 74(1):55-62

29 Löwenhielm P. (1975). Strain Tolerance of the Vv. Cerebri sup. (Bridging Veins) Calculated from Head-on Collision Tests with Cadavers. *Z. Reehtsmedizin.* 75(2):131-144

30 Löwenhielm P. (1978). Tolerance level for bridging vein disruption calculated with a mathematical model. *J Bioengineering* 2(6):501-507

31 Meaney DF. (1991). Biomechanics of acute subdural hematoma in the subhuman primate and man. University of Pennsylvania. PhD dissertation # AAI9125717

32 Lee MC, Haut RC. (1989). Insensitivity of tensile failure properties of human bridging veins to strain rate: implications in biomechanics of subdural hematoma*. J Biomechanics* 22(6-7): 537-42

33 Depreitere B, Van Lierde C, Sloten JV, Van Audekercke R, Van der Perre G, Plets C, et al. (2006). Mechanics of Acute Subdural Hematoma Resulting from Bridging Vein Rupture. *J Neurosurgery* 104(6):950–956

34 Melvin JW, Lighthall JW, Ueno K. (1993). Brain injury biomechanics, in Accidental Injury, eds Nahum A. M., Melvin J. W. (New York: Springer-Verlag;), 269–290

35 Caccese V, Lloyd J, Ferguson J (2014) An Impact Test Apparatus for Protective Head Wear Testing Using a Hybrid III Head-Neck Assembly. *Experimental Techniques.*

36 Lloyd J & Conidi F. (2015). Brain Injury in Sports. *Journal of Neurosurgery.* October.

37 Lloyd J. (2016). Biomechanics of Solo Motorcycle Accidents. *Journal of Forensic Biomechanics. 6:4.*

38 SAE (2013) J211/1. Instrumentation for Impact Test - Part 1 – Electronic Instrumentation. *Society of Automotive Engineers International*, Surface Vehicle Recommended Practice, Warrendale, PA.

39 Padgaonkar AJ, Krieger KW and King AI. Measurement of Angular Acceleration of a Rigid Body using Linear Accelerometers. *J Applied Mechanics*. Sept 1975.

40 Gadd CW. (1966). Use of a weighted-impulse criterion for estimating injury hazard. SAE Technical Paper, SAE Technical Paper 660793

41 Versace J. (1971). A review of the severity index, in: Proceedings of the 15th Stapp CarCrash Conference.

42 NHTSA. (2000). Final Economic Assessment, FMVSS No. 208 – Advanced Air Bags. Report # 1999-6407-0143.

43 Takhounts EG, Hasija V, Ridella SA, Tannous RE, et al. (2008). Investigation of Traumatic Brain Injuries Using the Next Generation of Simulated Injury Monitor (SIMon) Finite Element Head Model. Stapp Car Crash Journal 52: 1-32

44 Abbreviated Injury Scale (2008) Association for the Advancement of Automotive Medicine, Des Plaines, IL.

45 Prasad, P. Personal Communication

46 Prasad P and Mertz HJ. (1985). The position of the U.S. Delegation to ISO Working Group 6 on the Use of HIC in the Automotive Environment SAE technical paper 851246.

47 Prasad P, Barbat SD, Kalra A, Kim AS, et al. (2024). Evaluation of Brain Rotational Injury Criteria BrIC in vehicle frontal crashes. Traffic Injury Prevention 25 (1), 57-64.

48 Eppinger RH, Marcus JH, and Morgan RM. (1984). Development of dummy and injury index for NHTSA's thoracic side impact protection research program. SAE Technical Paper No. 840885.

49 Arora T, Zhang L and Prasad P. (2019). Development of a Subhuman Primate Brain Finite Element Model to Investigate Brain Injury Thresholds Induced by Head Rotation. Stapp Car Crash Journal, Vol. 63, pp65-82

50 Gabler LF, Crandall JR and Panzer MB. (2018). Development of a Metric for Predicting Brain Strain Responses. Ann. Biomed. Eng. 46(7):972–985.

51 Gabler LF, Crandall JR, and Panzer MB. (2018). Development of a Second-Order System for Rapid Estimation of Maximum Brain Strain. Ann. Biomed. Eng. 47(9):1971–1981

52 Newman JA, Shewchenko N, and Welbourne E. (2000). A proposed new biomechanical head injury assessment function— the maximum power index. Stapp Car Crash J. 44:215–247.

53 Kimpara H, and Iwamoto M. (2012). Mild traumatic brain injury predictors based on angular accelerations during impacts. Ann. Biomed. Eng. 40:114–126,

54 Yanaoka T, Dokko Y, and Takahashi Y. (2015). Investigation on an Injury Criterion Related to Traumatic Brain Injury Primarily Induced by Head Rotation. SAE Technical Paper 2015-01-1439.

55 Takahashi Y, and Yanaoka T. (2017). A Study of Injury Criteria for Brain Injuries in Traffic Accidents. 25th International Technical Conference on the Enhanced Safety of Vehicles, Detroit, MI.

APPENDIX

Table 1: Summary of motorcycle helmet test results (frontal impacts)

	N	Linear Velocity (m/s)	Linear Accel (g)	HIC_{15}	Impact Duration (msec)	Peak Impact Ang Vel (rad/s)	Peak Induced Ang Vel (rad/s)	Angular Accel (rad/s^2)	BrIC	AIS1 Mild concussion	AIS2 Severe concussion	AIS3 Serious Brain Injury	AIS4 Severe Brain Injury	AIS5 Critical Brain Injury
6D ATS-1R	15	11.6	124	696	24.7	26.5	36.0	5796	0.64	100.0	68.7	25.6	15.6	14.1
Bell DLX Mips	15	11.3	156	1089	16.3	20.3	40.9	5773	0.73	100.0	80.3	34.4	21.5	19.5
Bell Qualifier	9	10.4	184	1348	15.6	20.6	37.3	7572	0.66	100.0	71.9	27.7	16.9	15.3
Bilt Force	12	11.9	206	1701	15.2	24.3	36.1	6004	0.64	100.0	67.3	26.0	15.9	14.4
Bilt Vertex	6	11.9	132	913	16.3	27.9	36.3	5320	0.64	100.0	69.5	25.9	15.7	14.2
HJC i90	1	12.8	212	1508	15.8	16.9	38.5	10603	0.68	100.0	76.0	29.6	18.1	16.3
LS2 Stream EVO	2	12.7	170	1170	21.6	33.6	37.7	13673	0.67	100.0	74.0	28.2	17.2	15.5
Schuberth C2	2	12.4	146	1023	17.7	23.8	38.4	7341	0.68	100.0	75.9	29.5	18.0	16.3
Scorpion 400	2	13.3	208	1814	16.8	18.4	44.5	6525	0.79	100.0	88.4	41.1	26.0	23.6
Scorpion T510	7	10.8	126	742	19.3	23.3	47.0	4681	0.83	100.0	90.0	46.2	30.0	27.3
Shoei GT-air	2	12.6	159	1196	19.6	20.1	38.5	8526	0.68	100.0	76.1	29.7	18.2	16.4
Shoei Neotec	2	11.7	166	1099	14.3	35.8	38.3	7433	0.68	100.0	74.5	29.5	18.1	16.4
Shoei Neotec2	2	11.6	124	742	17.2	36.3	35.7	7138	0.63	100.0	67.8	24.8	15.0	13.6
Torq T-14	5	9.2	160	1204	16.3	18.9	37.6	4306	0.67	100.0	73.3	28.0	17.1	15.4
Arai Ram-X	2	11.9	198	1377	12.6	27.0	48.1	10180	0.85	100.0	93.2	48.4	31.4	28.6
Fulmer AF-35	2	12.7	293	2149	17.1	38.3	38.7	24859	0.68	100.0	76.2	29.8	18.2	16.5
Scorpion C220	11	11.7	239	1482	15.3	29.0	38.2	13076	0.68	100.0	72.9	29.7	18.4	16.7
Zox classic	3	17.2	266	2643	34.7	42.3	64.7	11086	1.15	100.0	99.8	78.4	58.3	54.3
Bell Pit Boss	14	11.2	209	1447	14.4	19.7	47.0	7546	0.83	100.0	90.6	46.1	29.8	27.2
Bell shorty	7	10.9	247	2062	13.2	29.1	45.0	12301	0.80	100.0	87.8	42.1	26.9	24.5
Daytona	2	12.5	401	3778	12.7	26.5	37.8	22307	0.67	100.0	74.2	28.3	17.2	15.6
Fulmer 305	2	12.5	355	2918	14.8	20.8	40.1	12909	0.71	100.0	80.0	32.7	20.2	18.3
HJC CS-2N	2	12.6	321	2435	14.3	21.8	39.7	17614	0.70	100.0	78.8	31.7	19.5	17.7
Outlaw shorty	2	9.8	163	1124	15.4	20.9	43.3	7107	0.77	100.0	85.5	39.0	24.6	22.3
Scorpion CT110	2	13.0	318	2114	16.3	25.1	39.9	20402	0.71	100.0	79.1	32.2	19.9	18.0
VCan V531	2	12.8	306	1909	16.2	21.2	41.0	19582	0.73	100.0	81.3	34.2	21.2	19.2
Zox micro	3	17.3	234	2547	25.8	39.2	70.1	10793	1.24	100.0	100.0	85.3	66.5	62.5
Gloss black	6	12.3	275	2047	13.9	50.5	37.6	29262	0.67	100.0	72.9	28.3	17.3	15.7
German style	5	9.6	396	3363	11.0	27.4	23.5	12201	0.42	100.0	29.8	8.4	4.9	4.4
Non-peak	5	10.0	714	9784	4.5	32.3	27.7	19357	0.49	100.0	42.9	14.1	8.4	7.6
Peak	4	8.6	457	3539	11.7	23.1	27.2	6745	0.48	100.0	41.3	12.8	7.5	6.8
Voss	6	8.7	591	5431	6.6	29.5	41.5	14014	0.74	100.0	80.2	35.7	22.6	20.5

Table 2: Summary of motorcycle helmet test results (occipital impacts)

	N	Linear Velocity (m/s)	Linear Accel (g)	HIC_{15}	Impact Duration (msec)	Peak Impact Ang Vel (rad/s)	Peak Induced Ang Vel (rad/s)	Angular Accel (rad/s^2)	BrIC	AIS1 Mild concussion	AIS2 Severe concussion	AIS3 Serious Brain Injury	AIS4 Severe Brain Injury	AIS5 Critical Brain Injury
6D ATS-1R	15	11.9	125	839	16.0	15.3	50.5	4308	0.90	100.0	95.1	53.2	35.1	32.1
Bell DLX Mips	20	11.3	162	1200	13.4	10.4	53.5	5822	0.95	100.0	96.9	58.9	39.9	36.6
Bell Qualifier	7	12.5	159	1328	14.9	22.8	52.8	5466	0.94	100.0	96.9	58.0	39.0	35.7
Bilt Force	12	10.7	127	731	15.5	4.3	51.6	6461	0.91	100.0	93.4	55.1	37.2	34.2
Bilt Vertex	6	10.7	124	729	14.3	3.7	46.3	5547	0.82	100.0	89.5	44.8	28.9	26.4
HJC i90	6	9.7	158	1031	12.4	8.8	51.6	7314	0.91	100.0	95.8	55.2	36.8	33.7
LS2 Stream EVO	2	12.2	135	1210	14.5	13.3	55.4	3455	0.98	100.0	98.2	62.6	42.9	39.4
Schuberth C2	2	10.7	196	1636	10.3	11.8	51.8	4478	0.92	100.0	96.3	55.7	37.0	33.9
Scorpion 400	2	12.6	214	1993	10.5	13.7	55.4	5599	0.98	100.0	98.2	62.6	42.9	39.4
Scorpion T510	13	11.4	171	1248	12.8	8.9	51.3	6190	0.91	100.0	95.5	54.6	36.3	33.3
Shoei GT-air	2	11.2	149	1085	15.0	23.3	47.5	4772	0.85	100.0	92.6	47.7	30.9	28.2
Shoei Neotec	2	10.9	163	1375	11.9	3.9	46.4	10504	0.82	100.0	91.1	44.8	28.7	26.1
Shoei Neotec2	2	10.3	151	1129	13.1	7.8	48.4	7346	0.86	100.0	93.2	48.9	31.8	29.0
Torq T-14	5	12.9	540	3345	23.1	42.8	28.1	21817	0.50	94.5	40.9	26.0	17.9	16.4
Arai Ram-X	2	11.2	158	1304	12.9	5.0	56.7	9072	1.01	100.0	98.3	65.0	45.2	41.6
Fulmer AF-35	2	12.2	173	1694	12.2	20.6	52.0	5446	0.92	100.0	96.4	56.1	37.4	34.2
HJC CS-5N	4	8.5	204	1137	11.7	4.8	54.5	9530	0.97	100.0	97.8	60.9	41.4	38.0
Scorpion C220	19	11.5	147	1004	14.7	15.9	53.2	4483	0.94	100.0	96.6	58.2	39.3	36.0
Shoei RJ-Air	4	8.0	236	1566	8.9	9.3	50.5	9581	0.89	100.0	95.3	53.0	34.9	31.9
Bell Pit Boss	20	11.1	180	1483	12.5	12.3	51.9	5240	0.92	100.0	95.6	55.7	37.2	34.1
Bell shorty	4	12.4	212	1832	11.6	25.8	46.3	6233	0.82	100.0	89.8	44.7	28.8	26.2
Daytona	6	13.0	307	2880	10.3	30.2	57.3	13759	1.03	100.0	97.4	65.3	46.8	43.4
Fuel shorty	3	13.6	244	2104	17.3	36.9	38.9	24587	0.69	78.6	62.8	40.8	29.2	27.1
Fulmer 305	2	11.5	231	2267	10.3	22.3	48.6	5067	0.86	100.0	93.2	49.2	32.0	29.2
HJC CS-2N	6	7.9	255	1281	9.6	11.8	46.4	5695	0.82	100.0	91.1	44.8	28.7	26.1
Outlaw shorty	2	13.2	484	3020	19.7	31.9	33.0	13315	0.58	99.7	51.3	30.5	20.5	18.8
Scorpion CT110	2	12.1	186	1668	12.3	18.8	52.3	4065	0.93	100.0	96.7	56.7	37.8	34.7
VCan V531	3	11.9	193	1546	12.2	24.5	47.9	5613	0.85	100.0	92.2	47.8	31.1	28.4
Gloss black	6	11.1	966	17704	3.1	35.7	44.4	20237	0.79	100.0	88.1	40.9	25.9	23.5
German style	5	11.8	672	8291	6.5	16.7	49.9	9087	0.88	100.0	94.1	51.8	34.1	31.2
Non-peak	10	9.6	731	10575	3.7	21.0	45.9	12232	0.81	100.0	90.3	43.9	28.0	25.5
Peak	6	12.2	824	13233	4.3	25.7	46.1	14077	0.82	100.0	90.3	44.2	28.3	25.8

Table 3: Summary of results across all unhelmeted tests

	N	Linear Velocity (m/s)	Linear Accel (g)	HIC_{15}	Impact Duration (msec)	Impact Ang Vel (rad/s)	Induced Ang Vel (rad/s)	Angular Accel (rad/s^2)	BrIC	AIS1 Mild concussion	AIS2 Severe concussion	AIS3 Serious Brain Injury	AIS4 Severe Brain Injury	AIS5 Critical Brain Injury
Mean	80	9.8	974	16230	2.4	26.7	40.6	18472	0.72	99.3	77.7	34.9	22.0	20.0
Standard Dev.		4.1	118	5078	0.5	17.9	8.3	14901	0.15	6.7	19.8	13.1	8.8	8.0

Table 4: Summary of results across all advanced motorcycle helmet tests

	N	Linear Velocity (m/s)	Linear Accel (g)	HIC_{15}	Impact Duration (msec)	Impact Ang Vel (rad/s)	Induced Ang Vel (rad/s)	Angular Accel (rad/s^2)	BrIC	AIS1 Mild concussion	AIS2 Severe concussion	AIS3 Serious Brain Injury	AIS4 Severe Brain Injury	AIS5 Critical Brain Injury
Mean	65	11.5	143	968	17.3	17.4	45.9	4564	0.81	100.0	86.2	44.3	28.9	26.4
Standard Dev.		1.7	29	332	5.5	8.9	8.0	1879	0.14	0.0	13.4	15.3	11.2	10.4

Table 5: Summary of results across all standard DOT motorcycle helmet tests

	N	Linear Velocity (m/s)	Linear Accel (g)	HIC_{15}	Impact Duration (msec)	Impact Ang Vel (rad/s)	Induced Ang Vel (rad/s)	Angular Accel (rad/s^2)	BrIC	AIS1 Mild concussion	AIS2 Severe concussion	AIS3 Serious Brain Injury	AIS4 Severe Brain Injury	AIS5 Critical Brain Injury
Mean	246	11.4	200	1494	14.7	19.5	46.3	6736	0.82	98.8	85.8	45.8	30.3	27.7
Standard Dev.		2.1	107	874	4.9	12.6	10.7	6409	0.19	9.9	18.8	17.2	12.9	12.0

Table 6: Summary of results across all novelty motorcycle helmet tests

	N	Linear Velocity (m/s)	Linear Accel (g)	HIC_{15}	Impact Duration (msec)	Impact Ang Vel (rad/s)	Induced Ang Vel (rad/s)	Angular Accel (rad/s^2)	BrIC	AIS1 Mild concussion	AIS2 Severe concussion	AIS3 Serious Brain Inj	AIS4 Severe Brain Inj	AIS5 Critical Brain Inj
Mean	53	10.4	641	8634	6.8	28.9	39.5	15435	0.70	100.0	73.4	33.1	21.0	19.1
Standard Dev.		1.8	244	6109	4.3	11.4	9.5	7488	0.17	0.0	24.4	15.7	10.5	9.7

Table 7: Comparison of results between DOT helmets, novelty helmets, and unhelmeted frontal impacts

	N	Linear Velocity (m/s)	Linear Accel (g)	HIC_{15}	Impact Duration (msec)	Impact Ang Vel (rad/s)	Induced Ang Vel (rad/s)	Angular Accel (rad/s^2)	BrIC	AIS1 Mild concussion	AIS2 Severe concussion	AIS3 Serious Brain Injury	AIS4 Severe Brain Injury	AIS5 Critical Brain Injury
Unhelmeted	9	9.1	985	17748	2.4	60.3	27.3	23277	0.48	100.0	42.3	13.6	8.1	7.3
Advanced DOT	30	11.4	140	893	20.5	23.4	38.5	3854	0.68	100.0	74.5	30.0	18.5	16.8
DOT full-face	52	11.4	168	1247	16.7	24.1	38.6	6488	0.68	100.0	74.2	30.3	18.8	17.0
DOT open-face	18	12.8	245	1738	18.4	32.1	43.8	12716	0.78	100.0	80.0	39.9	26.5	24.2
DOT half	36	12.0	252	1969	15.3	24.2	46.3	11242	0.82	100.0	87.2	44.2	29.2	26.7
Novelty	26	9.9	484	4798	9.5	33.5	32.3	17093	0.57	100.0	55.6	21.1	12.9	11.7

Table 8: Comparison of results between DOT helmets, novelty helmets, and unhelmeted occipital impacts

	N	Linear Velocity (m/s)	Linear Accel (g)	HIC_{15}	Impact Duration (msec)	Impact Ang Vel (rad/s)	Induced Ang Vel (rad/s)	Angular Accel (rad/s^2)	BrIC	AIS1 Mild concussion	AIS2 Severe concussion	AIS3 Serious Brain Injury	AIS4 Severe Brain Injury	AIS5 Critical Brain Injury
Unhelmeted	71	9.1	973	15565	2.4	20.2	43.6	12910	0.77	100.0	85.0	39.5	25.1	22.8
Advanced DOT	35	11.5	147	1033	14.6	12.3	52.3	5173	0.93	100.0	96.1	56.5	37.9	34.7
DOT full-face	61	11.3	185	1286	14.5	12.5	49.1	5689	0.87	99.5	90.1	51.7	34.5	31.6
DOT open-face	31	10.7	168	1157	13.3	13.2	53.1	6014	0.94	100.0	96.7	58.1	39.2	36.0
DOT half	48	11.6	228	1857	12.3	19.8	49.6	6626	0.88	98.7	90.8	52.4	35.2	32.3
Novelty	27	10.9	793	12327	4.2	24.5	46.4	13839	0.82	100.0	90.5	44.8	28.7	26.2

Table 9: Comparison of results between all DOT helmets, novelty helmets, and unhelmeted impacts

	N	Linear Velocity (m/s)	Linear Accel (g)	HIC_{15}	Impact Duration (msec)	Impact Ang Vel (rad/s)	Induced Ang Vel (rad/s)	Angular Accel (rad/s^2)	BrIC	AIS1 Mild concussion	AIS2 Severe concussion	AIS3 Serious Brain Injury	AIS4 Severe Brain Injury	AIS5 Critical Brain Injury
Unhelmeted	80	9.8	974	16230	2.4	26.7	40.6	18472	0.72	99.3	77.7	34.9	22.0	20.0
Advanced DOT	65	11.5	143	968	17.3	17.4	45.9	4564	0.81	100.0	86.2	44.3	28.9	26.4
DOT full-face	113	11.2	176	1257	15.4	17.7	43.9	5394	0.78	98.9	82.1	41.5	27.0	24.7
DOT open-face	49	11.2	192	1343	14.9	19.8	48.7	6902	0.86	98.0	88.7	50.4	33.9	31.0
DOT half	84	11.6	236	1883	13.4	21.4	47.6	8359	0.84	98.1	88.2	48.3	32.3	29.6
Novelty	53	10.4	641	8634	6.8	28.9	39.5	15435	0.70	100.0	73.4	33.1	21.0	19.1

Legend:	Unhelmeted (red)	Standard DOT - Full face (green)
	Advanced DOT-full face (dark blue)	Standard DOT - Open face (orange)
	Novelty (purple)	Standard DOT – Shorty (light blue)